CCSI Compressor

User Manual

Version 2.1.0

February 2025

Copyright Notice

License Agreement

Table of Contents

CCSI Compressor **1**

1.0 Reporting Issues 2

2.0 Version Log 2

Compressor Model **3**

1.0 Introduction 3

2.0 Compressor Stage Calculations 3

2.1 Dimensionless Numbers 4
2.2 Efficiency 5
2.3 Constraints 6

3.0 Multi-Stage Compressors 8

3.1 Integral Gear 8
3.2 Inline 8

4.0 TEG CO_2 Drier 9

5.0 Property Methods 10

5.1 Compression 10
5.2 Drying, Aspen Properties 12

6.0 ACM Model 14

6.1 Compressor Stage Calculations 14
6.2 Intercoolers 14
6.3 Multistage Compressor Models 15
6.4 Multistage Flash Model 15
6.5 Integral Gear Compressor with Drier Simulation 16
6.6 Inline Compressor with Drier Simulation 17

7.0 Results 18

7.1 Validation 18
7.2 Results for Typical Feed 19

8.0 Dynamic Simulations 22

8.1 Performance Curves 23
8.2 Surge Line 26

9.0 References 37

List of Figures

Figure 1: Maximum Mach number estimates. 7

Figure 2: ACM integral gear with drying flowsheet. 9

Figure 3: CO_2 saturated water content, Aspen Properties LK-PLOCK 11

Figure 4: CO_2 saturated water content, Aspen Properties HYSGLYCO 12

Figure 5: CO_2 solubility in TEG, Aspen Properties HYSGLYCO. 13

Figure 6: ACM flowsheet for an integral gear compressor with drier. 16

Figure 7: ACM flowsheet for an inline compressor with drier. 17

Figure 8: Dimensionless performance curves for Stage 1. 25

Figure 9: ACM dynamic simulation example: Ramp change in inlet flow rate, pressure plot. 30

Figure 10: ACM dynamic simulation example: Ramp change in inlet flow rate, flow rate plot. 30

Figure 11: ACM dynamic simulation example: Ramp change in inlet flow rate, temperature plot. 31

Figure 12: Dynamic simulation example: Ramp change in inlet flow rate, electric power plot. 31

Figure 13: Specification box for compressor model. The process flowsheet model "CO2_process_flowsheet_full" is highlight in the "project tree" menu on the left. Note: Specifying the required variables is done by double-clicking each piece of process equipment under the "Topology" tab of the "CO2_process_flowsheet_full" window. These values are set to default values. 32

Figure 14: Click "Play" (the green arrow on the top toolbar while the "CO2_process_flowsheet_full Model" window is open). This opens the "Simulate" window. The "Initialisation Procedure" drop-down menu enables the user the option to run the initialization procedure. 33

Figure 15: Data selection window for gRMS template. 34

Figure 16: gPROMS dynamic simulation example: Ramp change in inlet flow rate, pressure plot. 35

Figure 17: gPROMS dynamic simulation example: Ramp change in inlet flow rate, flow rate plot. 35

Figure 18: gPROMS dynamic simulation example: Ramp change in inlet flow rate, temperature plot. 36

Figure 19: gPROMS dynamic simulation example: Ramp change in inlet flow rate, electric plot. 36

List of Tables

Table 1: Maximum Stage Mach Numbers 6

Table 2: Comparison of Property Methods 10

Table 3: Compressor Specifications 18

Table 4: Comparison of Simulations to Compressor Quotes 19

Table 5: Solid Sorbent Capture, CO_2 Stream Conditions 19

Table 6: Compressor Comparison Summary 20

Table 7: Integral Gear Compressor Stage Summary 20

Table 8: Inline Compressor Stage Summary 21

Table 9: Estimated Parameters for Stage 1 24

Table 10: Estimated Parameters for Correlation 21 25
Table 11: Estimated Parameters for Stages 3, 5, and 7 26

To obtain support for the products within this package, please send an e-mail to ccsi-support@acceleratecarboncapture.org.

CCSI Compressor

Multi-stage Centrifugal Compressor Model: A unified set of compressor models including steady-state design point model and dynamic model with surge detection.

1.0 REPORTING ISSUES

To report an issue, please send an e-mail to ccsi-support@acceleratecarboncapture.org.

2.0 VERSION LOG

Product	Version Number	Release Date	Description
CO_2 Compressor Simulation	2.1.0	2/28/2025	Previous ACM model has now been upgraded to Aspen V14.
CO_2 Compressor Simulation	2.0.0	3/31/2018	Initial Open Source release
CO_2 Compressor Simulation	2015.10.0	10/31/2015	Bug fixes and added gPROMS model
CO_2 Compressor Simulation	2014.10.0	10/31/2014	Previous ACM model has now been upgraded to Aspen V8.4.

Compressor Model

1.0 INTRODUCTION

This manual presents information on the CO_2 compression system that uses a train of multistage integral gear compressors to compress the CO_2-rich gas from the regenerator to the supercritical phase for pipeline transport. In this work, the design point size and performance of the integral gear compressors are validated with the design data provided by the commercial vendor. For simulating off-design performance of the compressor, the performance curves obtained from a commercial vendor are leveraged. Interstage coolers, flash vessels, recycle loops, glycol tower for water removal, and the inventory of the associated system significantly affect the performance and transient response of the compression system. To capture the effect of this associated system, a pressure-driven dynamic model of the entire system is developed using Aspen Custom Modeler® (ACM) and gPROMS®. Surge must be avoided during operation of the centrifugal compressors to avoid significant damage to the compressor and the associated equipment. To this end, a surge detection algorithm has been developed. For avoiding surge, the compressor system should be appropriately developed and control action must be taken. Gain-scheduling controllers are designed to move the compressor away from the surge conditions. The dynamic model is used to study the transients of the key variables in response to various disturbances such as change in the flow rate, temperature, and composition of the feed to the compression system.

2.0 COMPRESSOR STAGE CALCULATIONS

This document describes a method for predicting the design point centrifugal compressor performance. An ACM implementation is provided. ACM Version 8.4 or higher is required. The compressor model and design constraints are taken mainly from Angier (2000) and Lüdtke (2004). The methods were validated as much as possible by comparison to typical industrial compressors. The purpose of the compressor modeling work is to provide simple compressor equations that can be used in the optimization of CO_2 capture and compression systems. The compressor model uses preliminary design calculations and does not require any detail about the compressor geometry, making it relatively easy to use. Multi-stage compressor models are provided that include TEG drying systems. This section describes the basic design point calculations for centrifugal compressor stages.

2.1 Dimensionless Numbers

The calculations are based on dimensionless numbers that characterize a compressor stage. This section provides the definitions for important dimensionless numbers.

The mass flow coefficient (φ) is given by Equation 1 where $\dot{m}$ is the mass flow rate in kg/s, ρ_0 is the density at the stage inlet in kg/m^3, r_2 is the impeller radius in m, and U_2 is the speed of the impeller tip in m/s.

$$\varphi = \frac{\dot{m}}{\pi \rho_0 r_2^2 U_2} \tag{1}$$

The polytrophic head coefficient (μ_p) is given by Equation 2, where Δh_p is the polytropic enthalpy change through the compressor stage in J/kg. Head units of m^2/s^2 are equivalent to J/kg.

$$\mu_p = \frac{\Delta h_p}{U_2^2} \tag{2}$$

The work coefficient (I) is similar to the polytropic head coefficient, but it uses the actual enthalpy change instead of the polytropic enthalpy change. The work coefficient is given by Equation 3.

$$I = \frac{\Delta h_t}{U_2^2} \tag{3}$$

The rotational Mach number (Ma) is the primary factor in determining the pressure ratio for a stage. Higher Ma numbers result in less stable operation, so stages with higher Ma can operate over a smaller range of inlet conditions. The Ma number is given by Equation 4, where a_0 is the speed of sound in the gas at the compressor inlet.

$$\mathrm{Ma} = \frac{U_2}{a_0} \tag{4}$$

The speed of sound in a gas is given by Equation 5, where P is pressure, ρ is mass density, and s is entropy. The equation can be converted into a slightly more useful form, where κ_T is the isothermal compressibility, c_p is the constant pressure heat capacity, and c_v is the constant volume heat capacity. Some property packages may calculate speed of sound or isothermal compressibility directly.

$$a = \sqrt{\left(\frac{\partial P}{\partial \rho}\right)_s} = \sqrt{\left(\frac{c_p}{c_v}\right)\frac{V}{M\kappa_T}} = \sqrt{\left(\frac{c_p}{c_v}\right)\frac{1}{\rho\kappa_T}} \tag{5}$$

2.2 Efficiency

With the above dimensionless numbers, efficiency can be estimated. Two types of efficiencies are commonly used, adiabatic and polytropic.

Adiabatic efficiency is calculated by first calculating the isentropic enthalpy change between the inlet conditions (P_0, T_0) and the outlet conditions (P_2, S_0) (the isentropic discharge temperature is not the actual discharge temperature). Dividing the isentropic enthalpy change by the actual change in enthalpy between the inlet conditions (P_0, T_0) and the outlet conditions (P_2, T_2) gives the adiabatic efficiency. The adiabatic efficiency is easy to calculate but has the disadvantage that it depends on the pressure ratio of the compressor, making it more difficult to interpret.

Polytropic efficiency is more convenient because it is independent on pressure ratio. The polytropic head is calculated over a reversible path of constant efficiency. Equation 6 provides a very good approximation for polytropic enthalpy change in a real gas (Mallen and Saville, 1977). In Equation 6, temperature is in K.

$$\Delta h_p = \Delta h_t - \frac{(\Delta s)(\Delta T)}{ln\left({T_{out}}/{T_{in}}\right)} \tag{6}$$

The polytropic efficiency is given by Equation 7.

$$\eta_p = \frac{\Delta h_p}{\Delta h_t} = \frac{\mu_p}{I} \tag{7}$$

Compressor stage efficiency can be related to the flow coefficient. Aungier (2000) gives correlations between the flow coefficient and the polytropic and work coefficients. These empirical correlations are for typical well designed centrifugal compressors. The correlations are given by Equations 8 and 9 for covered impellers with vaned diffusers, and Equations 10 and 11 for open impellers with vaned diffusers.

$$I = 0.62 - \left({\varphi}/{0.4}\right)^3 + {0.0014}/{\varphi} \text{ (covered)} \tag{8}$$

$$\mu_p = 0.51 + \varphi - 7.6\varphi^2 - {0.00025}/{\varphi} \text{ (covered)} \tag{9}$$

$$I = 0.68 - \left({\varphi}/{0.37}\right)^3 + {0.002}/{\varphi} \text{ (open)} \tag{10}$$

$$\mu_p = 0.59 + 0.7\varphi - 7.5\varphi^2 - {0.00025}/{\varphi} \text{ (open)} \tag{11}$$

Covered impellers add weight, but do not require the tight tolerances of open impellers. In small stages, covered impellers may be used since relatively tight tolerances become more difficult to achieve.

2.3 Constraints

This section presents design constraints for centrifugal compressors. These constraints are approximate and vary depending on the manufacturer. The constraints presented here should provide a good approximation for generic compressor cases.

The mass flow coefficient for centrifugal compressors is usually between 0.01 and 0.15 (Lüdtke, 2004).

Limits on Ma for multistage compressors are given by Equation 12, where n is the stage number. Equation 12 is based on Lüdtke (2004). The limits on Ma are dependent on more detailed design considerations, so the limits given by Equation 12 are approximate. Since high Ma numbers reduce the allowable range of operating conditions, it makes sense that earlier stages can have higher Ma numbers since pressure variations will be magnified through each stage.

$$\mathrm{Ma} \leq -0.202 \ln(n) + 1.25 \tag{12}$$

Table 35 shows the Ma limits from Equation 12 for easy reference.

Table 1: Maximum Stage Mach Numbers

Stage	Ma_{max}	Stage	Ma_{max}
1	1.25	8	0.83
2	1.11	9	0.81
3	1.03	10	0.78
4	0.97	11	0.77
5	0.92	12	0.75
6	0.89	13	0.73
7	0.86	14	0.72

If Equation 12 is applied to the stages of an integral gear compressor, the Ma numbers calculated from a typical industrial integral gear compressor can be compared. Figure 69 shows the result. The low estimate and high estimate are from Lüdtke (2004). The average estimate curve is Equation 12, and the purple dots are compressor data. It can be seen from Figure 69 that it seems likely that Ma number limits, similar to those in Equation 12, were taken into account in the industrial compressor design. Other constraints, which will be discussed, may affect the first and last stages.

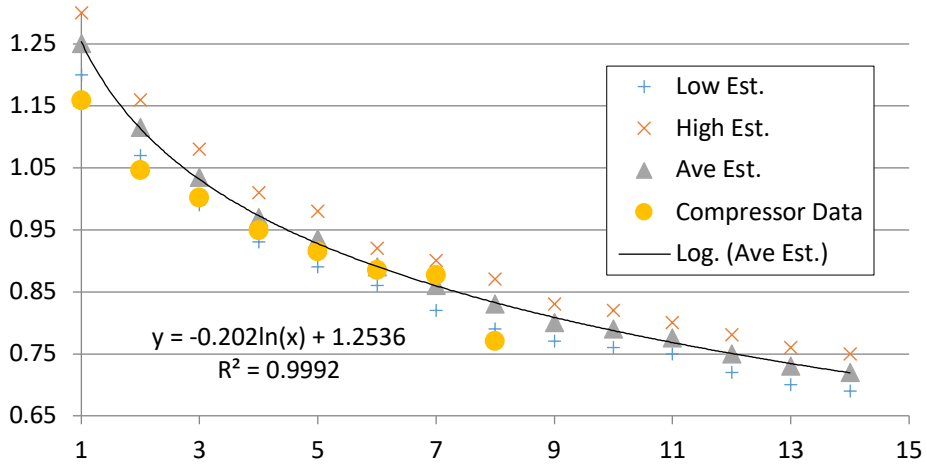

Figure 1: Maximum Mach number estimates.

The impeller tip speed is limited by maximum stress on the impeller. Equation 13 was adapted from Lüdtke (2004) for steel impellers, where U_2 is the impeller tip speed in m/s, and $R_{P0.2}$ is the yield stress of the material in MPa. For typical impellers, $R_{P0.2} \approx 830$ MPa, although there are higher strength steels (Lüdtke, 2004). The maximum tip speed allows stress in the impeller up to 70% of the yield stress.

$$U_2 \leq \sqrt{0.7(1984.1\varphi^2 - 616.88\varphi + 215.97)R_{P0.2}} \tag{13}$$

Comparing Equation 13 to the calculated tip speed from the first stage of the industrial compressor shows a tip speed of 312 m/s and a maximum tip speed given by Equation 13 of 314 m/s. It seems that this may be an active constraint in some compressor designs.

The rotational speed of a centrifugal compressor is limited to approximately 20,000 rpm or 25,000 rpm for very high speed compressors (Lüdtke, 2004). The last stage in the industrial compressor has a rotation speed of 24,743 rpm. From Figure 69 it can be seen that the Ma number for the last stage is significantly below the trend set by the other stages. This may be because it is constrained by maximum rotation speed instead of maximum Ma. In this work, the maximum rotation speed of 20,000 rpm will be applied to inline compressors. The 25,000 rpm limit will be applied to integral gear and single stage compressors.

The discharge temperature of a stage is generally limited to less than 250°C (482°F). Temperatures of 250°C or greater are possible but may require special construction (Lüdtke, 2004). Other temperature limits apply depending on the gas being compressed, but are probably not of concern in the CO_2 application.

Stage diameters are generally between 150 mm and 1,500 mm, although it depends on the manufacturer. Some manufacturers may make stages with diameters up to 2,000 mm (Lüdtke, 2004).

For this work, impellers with a diameter of less than 400 mm were assumed to be covered impellers, and larger impellers were assumed to be open. This is still a matter for further study.

3.0 MULTI-STAGE COMPRESSORS

There are two basic compressor designs considered in this work, integral gear and inline.

3.1 Integral Gear

The integral gear compressor offers high efficiencies and relatively low power requirements. The integral gear design consists of pairs of stages arranged around a central gear. Both stages in a pair operate at the same speed but can have different diameters. Since the rotation speed changes after every other stage, stages can operate near their optimum efficiency. The arrangement of an integral gear compressor also allows intercooling after every stage, which significantly reduces the power requirements. At high pressure, intercooling is reduced or not used at all to avoid liquefaction of CO_2. Due to the intercooling, temperatures do not generally get high enough to recover compression heat for use in other parts of the process.

3.2 Inline

The inline compressor contains sections of compressor stages in the same casing which run on a common shaft. Stages in a section have the same radius and run at the same speed. Since several stages operate at the same speed, some stages may operate far from the optimal mass flow coefficient, resulting in lower efficiencies than integral gear compressors. Intercooling also happens between sections, so there are fewer intercoolers than in an integral gear compressor; however, higher temperatures increase heat integration opportunities. Gear boxes can help different sections of an inline compressor to operate at different speeds.

4.0 TEG CO_2 DRIER

The bituminous baseline report specifies the maximum water content for CO_2 as 150 ppm, so a drying system is required (U.S. Department of Energy, 2010). The triethylene glycol (TEG) drying system was modeled. Figure 70 shows the layout of the drying system in an integral gear compressor. The absorber and regenerator consist of packed columns. The columns are modeled using a series of flash blocks to simulate equilibrium stages.

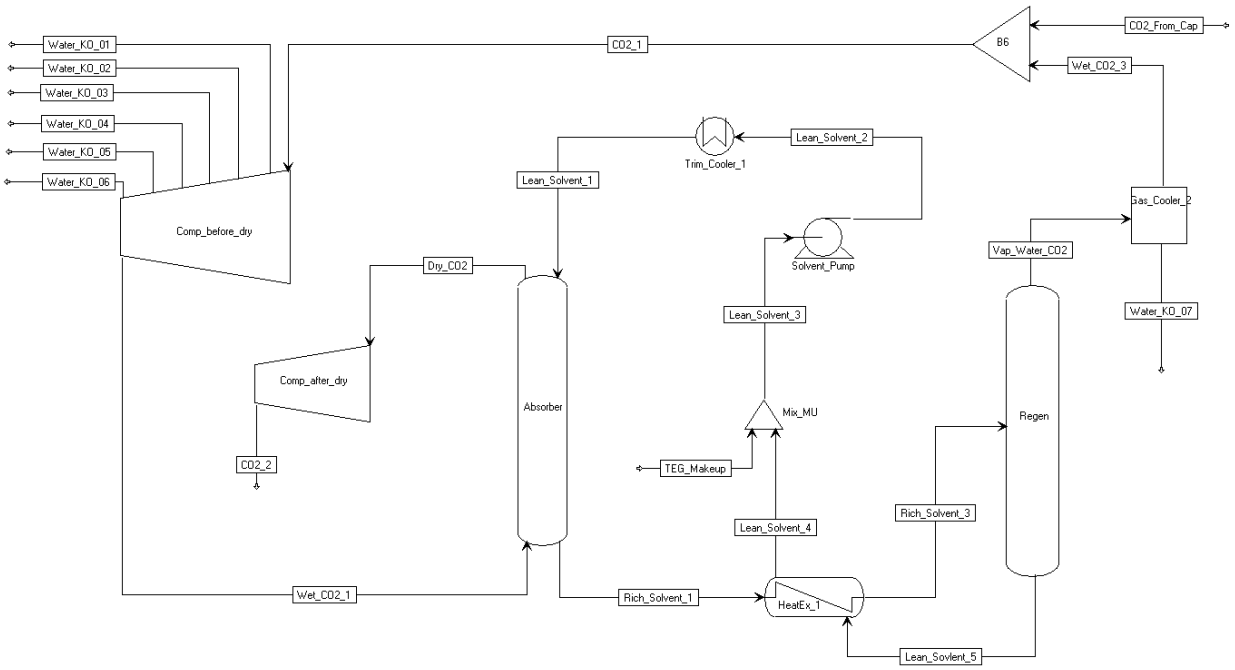

Figure 2: ACM integral gear with drying flowsheet.

Lean (low CO_2 and water content) TEG solvent flows into the top of the absorber, and wet CO_2 flows into the bottom. TEG absorbs both water and CO_2 from the CO_2 phase. The absorber operates at a pressure of about 45 to 60 bar. Approximately four times more CO_2 is absorbed than water on a mole basis. The gas phase pressure drop in the TEG absorber column was assumed to be 5 psia, although this value was based on a concurrent contactor (Kohl and Nielson, 1997). The pressure drop depends on the packing used, so other systems may have lower pressure drops. This is still a matter for further study.

CO_2 leaves the absorber with a water content of 150 ppm, and continues on to be compressed further. The rich solvent leaving the absorber goes to a heat exchanger where it gets heated by the lean solvent leaving the regenerator.

The rich solvent is fed to the regenerator, which operates at a pressure of about 1 to 2 bar. The regenerator also contains a reboiler. Due to the lower pressure in the regenerator, most of the water and CO_2 are desorbed from the TEG solvent, and very little heat is required. The CO_2 phase released from the solvent flows through a condenser where most of the TEG and water are removed. The low pressure CO_2 saturated with water is recycled back to the compressor feed. About 2 to 3% of the CO_2 feed is recycled for a typical configuration.

5.0 PROPERTY METHODS

There are two main parts of the compressor simulation, compression and drying. The compression section requires accurate properties for CO_2 to predict compressor power. The drying section requires accurate vapor-liquid equilibrium calculations for the CO_2-TEG-Water system.

5.1 Compression

Most property methods provide a good approximation of the properties of CO_2 over a wide range of temperatures and pressures, but have relatively large errors near the critical point. For the compressor, this potentially leads to power calculations that can have significant error. The Span-Wagner property method provides a highly accurate property method for CO_2 (Span and Wagner, 1996); however, it cannot be used for mixtures in Aspen Properties (in Aspen it is available as REFPROP). To find the best method, other equations of state were compared to Span-Wagner. Table 36 shows the results for conditions similar to a compressor stage with the least accurate results.

Since Span-Wagner cannot be used because of water in the CO_2 stream, the Lee-Kesler-Plöcker (LK-PLOCK) appears to provide the next best method.

The property method for the compressor sections of the flowsheet is also used to calculate water knockout in the intercoolers. Figure 71 compares the LK-PLOCK predictions to experimental data. The data in Figure 71 approximately covers the range that would be found in the intercoolers. The 25° and 31.04°C curves are shorter because the flash calculation failed at higher pressures for those temperatures. While the fit is probably acceptable, improvements may be made by adjusting the model parameters in future work.

Table 2: Comparison of Property Methods

(T_1 = 55 °C, P_1 = 55 bar) and (T_2 = 109 °C, P_2 = 100 bar) Pure CO_2		
	Δ (kJ/kmol)	**Relative Error (%)**
Aspen Ideal	2154.4	38.7
Aspen BRWS	1582.0	1.8
Aspen BWR-LS	1558.1	0.3
Aspen LK-PLOCK	1556.5	0.2
Aspen Refporp (Span-Wagner)	1553.7	0.0
NIST Refprop (Span Wagner)	1553.7	0.0
Handbook (Span-Wagner)	1553.7	0.0
Aspen/Hysis SRK	1502.4	-3.3
Aspen RKS	1498.3	-3.6
Aspen SRK	1494.0	-3.8
Aspen RKS-BM	1451.2	-6.6
Aspen RK-ASPEN	1451.2	-6.6
Aspen SR-Polar	1451.2	-6.6
Aspen/Hysis Peng-Robinson	1447.2	-6.9
Aspen Peng-Robinson	1442.8	-7.1

(T_1 = 55 °C, P_1 = 55 bar) and (T_2 = 109 °C, P_2 = 100 bar) Pure CO_2		
	Δ (kJ/kmol)	Relative Error (%)
Aspen/Hysis Glycol	1429.7	-8.0
Aspen Grayson2	1426.4	-8.2
Aspen PR-BM	1395.1	-10.2

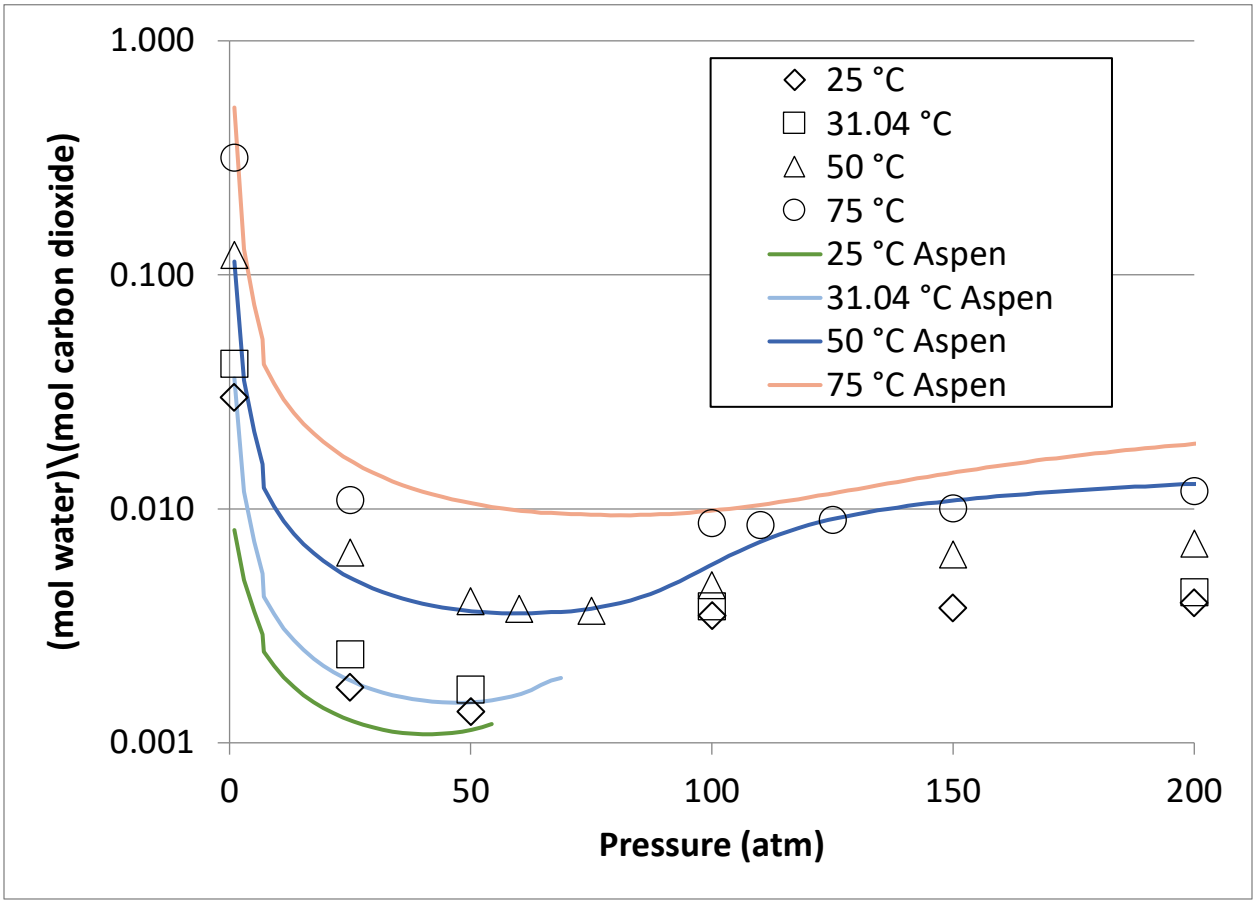

Data Source: Wiebe and Gaddy (1941)

Figure 3: CO_2 saturated water content, Aspen Properties LK-PLOCK.

5.2 Drying, Aspen Properties

The drying section of the flowsheet makes use of an Aspen Properties method named HYSGLYCO, which is specially designed to work for drying natural gas with TEG. CO_2 is a component of natural gas, but in low concentrations.

This section provides some comparisons between Aspen Properties predictions and literature data. Figure 72 shows the predictions for saturated water content of CO_2 in a CO_2/water system. The HYSGLYCO method provides better agreement than LK-PLOCK, and appears to be reasonably accurate, although there is a discontinuity in the 25° and 31.04°C curves.

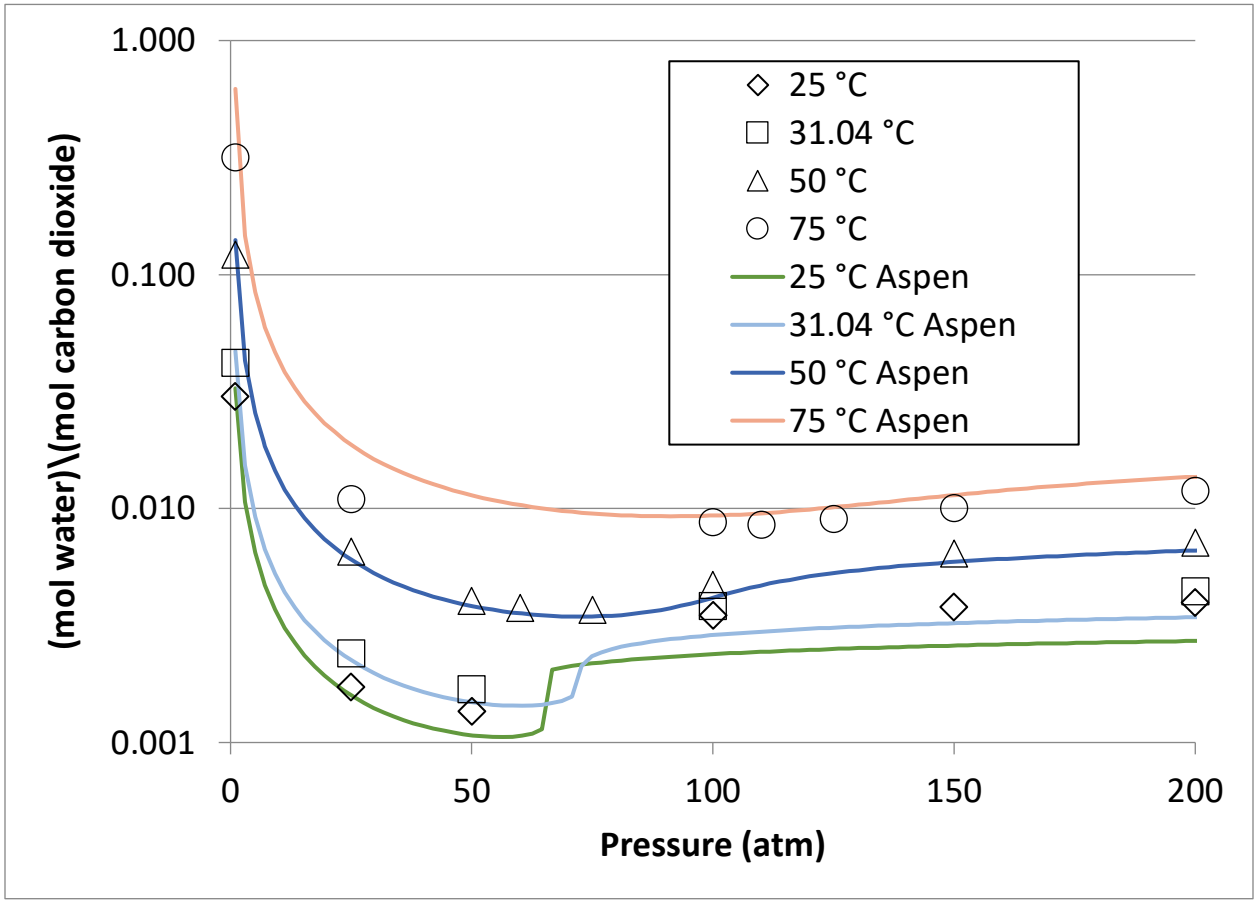

Data Source: Wiebe and Gaddy (1941)

Figure 4: CO_2 saturated water content, Aspen Properties HYSGLYCO.

Figure 73 shows the solubility of CO_2 in TEG calculated by Aspen compared to literature data.

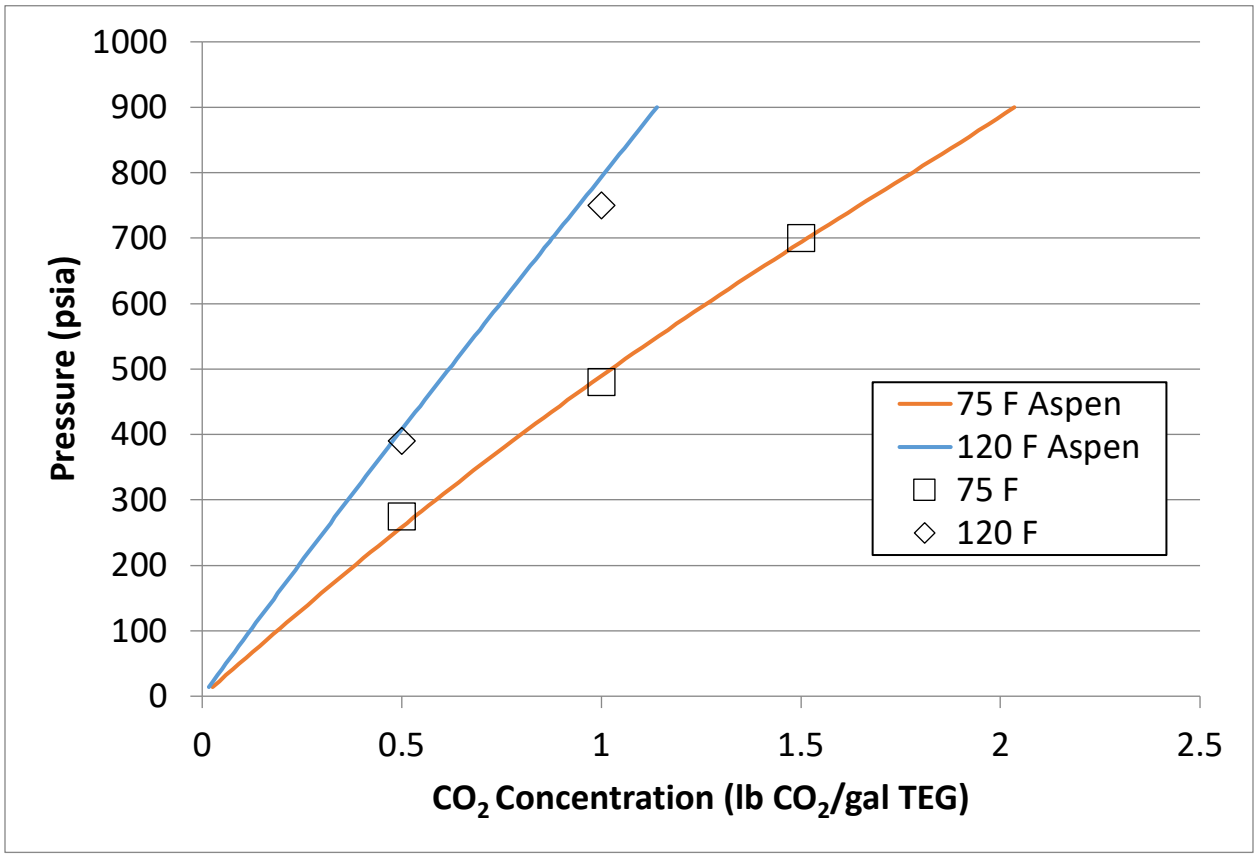

Data Source: Kohl and Nielson (1997)

Figure 5: CO_2 solubility in TEG, Aspen Properties HYSGLYCO.

The property methods chosen for the compressor simulation probably provide reasonable approximations; however, some refinement may be able to yield better results. The current property method selection provides the best results obtainable with standard Aspen provided parameters. The collection of additional data and refinement of parameters is a matter for future work. Additionally, since HYSGCLYCO is not available in Multiflash, the gPROMS process model uses the less accurate LK-PLOCK method.

6.0 ACM MODEL

This section describes ACM compressor model implementation. Two ACM files are provided. The file "CompIG.acmf" provides a simulation for an integral gear compressor and drier. The file "CompInline.acmf" provides a simulation of an inline compressor and drier.

6.1 Compressor Stage Calculations

There are two models for centrifugal compressor stages. The first is a simple stage calculation (CompStageSimple), which uses a specified efficiency to do the compressor stage calculation.

The second compressor model (CompStagePrelimDesign) uses the calculations detailed in this document to estimate the performance of compressor stages. Assuming the inlet stream for a stage is specified, this model has two degrees of freedom. The list below provides variables typically specified for a stage, two of which should be fixed. Some variables are mutually exclusive, e.g., discharge pressure and pressure ratio.

- Mass flow coefficient (phi)
- Polytropic head coefficient (mu_p)
- Work coefficient (I)
- Rotational Mach number (Ma)
- Pressure ratio (Pratio)
- Discharge pressure (i_port.P)
- Tip speed (U2)
- Rotation speed (rspeed)
- Impeller radius (r2)

There are also several parameters that define characteristics of the compressor stage.

- Diffuser type (diffuser_type)
- Impeller type (impeller_type)
- Driver efficiency (eff_drive)
- Mechanical efficiency (eff_mech)

The variables that should be fixed depend on the compressor configuration.

6.2 Intercoolers

The intercoolers are modeled as flash stages using the "Flash_Stage" model, which is provided in the ACM files. Assuming the inlet stream is known, the flash stage has two degrees of freedom. For intercoolers, temperature and pressure are usually fixed. A pressure drop at the flowsheet level can be used to set the discharge pressure of a flash stage. To set the temperature and pressure, fix the temperature and pressure of either the liquid or vapor outlet port. The liquid stream is the water knockout.

6.3 Multistage Compressor Models

There are two multistage compressor models ("CompInline" and "CompIntegralGear") provided in the ACM files. Both models include an array of compressor stages. The integral gear compressor model contains a series of compressor stages, and each stage is followed by an intercooler. An intercooler may be disabled by setting the heat flow and pressure drop to zero. The inline compressor model contains only a series of compressor stages and no intercoolers.

Multiple multistage models can be combined to form a complete compressor model. For inline compressors, two or three inline sections may be separated by intercoolers. For integral gear compressors, there may be a compressor section before and after a drier.

The multistage compressor models calculate the maximum impeller tip Ma number for each stage. Both multistage models have a parameter that allows the first stage number to be set. If a compressor model is made of several multistage sections, this can be used so the models know the correct stage number.

Several special forms for the multistage compressor models make it easier to find variables.

- Dimensionless – mass flow coefficients for each stage
- Efficiency – polytropic, adiabatic, driver, and mechanical efficiencies for each stage
- Impeller_Diffuser – the impeller and diffuser type for each stage
- Power – fluid and electric power for each stage
- Speed – rotation speed, tip speed, and Ma for each stage, as well as limits for Ma and tip speed
- TPQ – temperature, pressure, and heat transfer into and out of each stage and intercooler, as well as pressure drop, for intercoolers in integral gear models

The integral gear model sets the rotation speed of the even numbered stages to be equal to the odd stage before them. This leaves the odd stages with two degrees of freedom and the even stages with one. The mass flow coefficient can be set in the odd stages to provide near optimal efficiency. The impeller tip speed or Ma numbers can get the desired discharge pressure. The constraints listed in Section 2.3 Constraints must be checked to ensure the result is feasible. Pressure ratio can be increased at the expense of efficiency by lowering mass flow coefficients. If the desired outlet pressure cannot be achieved without violating constraints, the number of stages must be increased. The intercoolers are specified by a pressure drop and temperature. If an intercooler is not needed at a particular location, the heat flow and pressure drop can be set to zero.

The inline model sets the radius and rotation speed of all stages equal to the first stage. Only the first stage has two degrees of freedom, and the rest are specified by that. An inline compressor can be constructed of multiple inline models with intercoolers between.

6.4 Multistage Flash Model

The multistage flash models are used to simulate equilibrium stages for separation columns. The number of stages is a parameter in the model. Inlets can be added to any stage, and there is a gas outlet at the first (top) stage and a liquid outlet at the last (bottom) stage. A stage can act as a reboiler or condenser by setting the temperature or heat flow for the stage. Most stages will be adiabatic so the heat flow can be set to zero. To get the flash stages to converge for the first time, it is better to fix the temperature. After the model converges with the fixed temperature, the temperature variable can be freed and the heat transfer can be fixed.

6.5 Integral Gear Compressor with Drier Simulation

Figure 74 shows the ACM flowsheet for the integral gear compressor with a TEG drier, which is contained in the "CompIG.acmf" file.

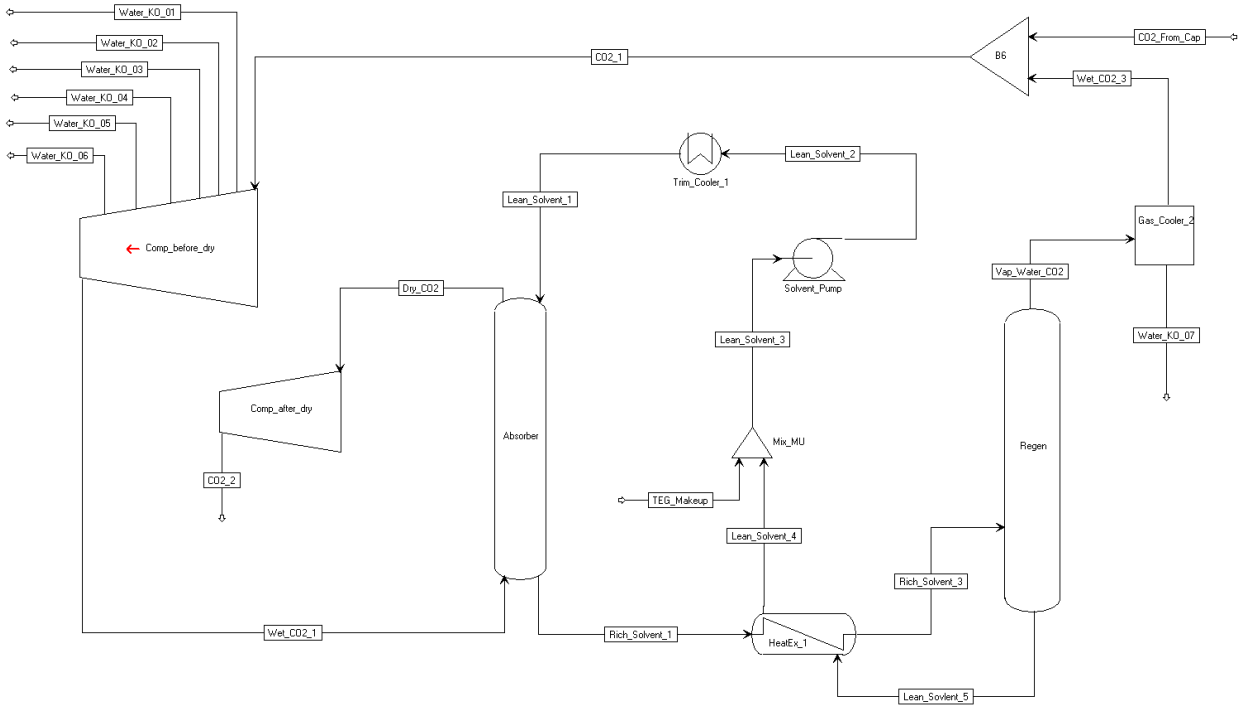

Figure 6: ACM flowsheet for an integral gear compressor with drier.

The flowsheet consists of two compressor sections with a TEG drying system between. The simulation is configured for a typical CO_2 stream from a solid sorbent process. The flow rate is about half the CO_2 captured from a 650 MW power plant at 90% capture; this size of compressor would be commercially available.

The first compressor section consists of six stages with intercooling after each stage. Water knockout streams are attached to each intercooler. The second compressor section after the drier has two stages and no intercooler. There is an after-cooler after the last stage, which should supply enough heat for the regenerator in the drying system.

The mass flow coefficients for the odd compressor stages were set to 0.09, providing good efficiency and allowing pressure ratios high enough to obtain the required discharge pressure of 2216 psia. The first compressor stage speed is limited by stress on the impeller. The remaining stage speeds are limited by the impeller tip Ma number. To determine the tip speed for the first stage and Ma for the remaining stages, equations at the flowsheet level were used that set the tip speed or Ma equal to some fraction of their maximum. The fraction was determined to produce the correct discharge pressure. In this case, the fraction for first-stage tip speed and Ma for the rest of the stages was 0.9965. If the fraction is greater than 1, there is a constraint violation. Either the mass flow coefficients can be lowered or more stages can be added if needed.

The flowsheet variables “teg_flow” and “water_content” are used to control the water content of the CO_2 leaving the compressor. The TEG solvent flow rate is calculated to get the desired water content. The CO_2 pressure into the absorber column is about 860 psia in this case. In the absorber, the CO_2 and water are absorbed by the TEG solvent. The absorber consists of five equilibrium stages.

After leaving the absorber, the rich solvent gets heated by the lean solvent leaving the regenerator. The rich solvent is fed directly to the reboiler, which is operated at 250°F and 16 psia. The large pressure drop causes CO_2 and water to be desorbed from the solvent. Only one equilibrium stage is required for the regenerator. The regenerator contains two stages, but the second stage does not do anything. The CO_2 and water then go to a condenser where most of the water is removed, and the saturated CO_2 is recycled to the compressor inlet. Some TEG is lost in the drying process, so there is a TEG make-up stream.

6.6 Inline Compressor with Drier Simulation

Figure 75 shows the ACM flowsheet for the inline compressor with TEG drier simulation, which is contained in the “CompInline.acmf” file.

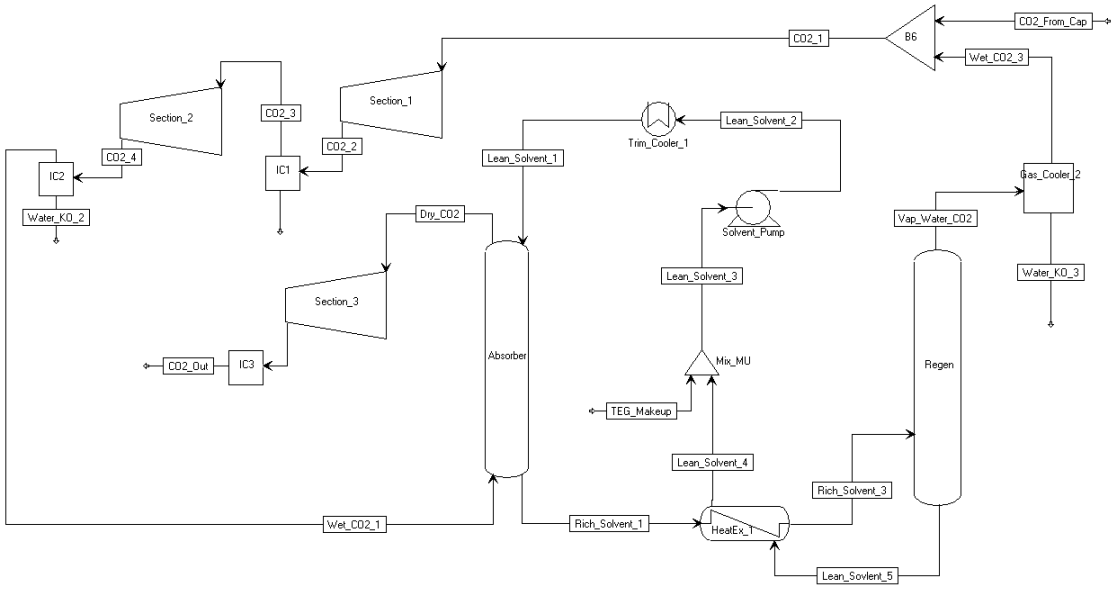

Figure 7: ACM flowsheet for an inline compressor with drier.

The inline compressor model has the same drying section as the integral gear compressor, but the absorber operates at 710 psia due to its placement in the compressor train. The feed is the same as the integral gear model.

The inline compressor consists of three inline sections. The first section has three stages, the second section has four stages, and the third section after the drier has three stages. There are no intercoolers in inline sections, but there are intercoolers between sections. A gear box between each section allows them to operate at different speeds. The mass flow coefficient for the first stage in each section was set to 0.11, 0.12, and 0.12. The higher mass flow coefficients provide a better efficiency over the whole section.

The compressor speed in the first section is limited by impeller stress. The speed of the second section is limited by the Ma number, and the last section is limited by the maximum rotation speed. The rotation speed of the last section is set to 20,000 rpm. The first and second sections are set to a fraction of the maximum impeller tip speed and Ma number respectively. The fraction of the maximum is calculated to produce the required discharge pressure. The fraction is 0.9964.

7.0 RESULTS

This section provides some simulation results. First, the simulation results are validated by comparison to typical industrial compressors. Then results for the integral gear and inline compressor configurations are compared for a typical CO_2 stream from a solid sorbent process.

7.1 Validation

The compressor model was validated by comparing results to typical industrial integral gear compressors. Four compressors were examined and are summarized in Table 37. The comparison was done in two ways. First (case a), the results were compared with the model compressor stages set to the same diameter and rotation speed as the compressor quotes; in this case, the discharge pressure from the simulation does not necessarily match the quote. In the second comparison (case b), a compressor was designed to produce the specified outlet pressure by setting the mass flow coefficient of every other stage and setting the Ma number of each stage to some fraction of the maximum, which was determined to produce the required discharge pressure; in this case, the rotation speed and diameter do not necessarily match the quotes. Information about intercooling in the last one or two stages was incomplete, which has some effect on the results, most significantly on the discharge temperatures.

Table 3: Compressor Specifications

Compressor	Inlet Pressure (psia)	Number of Stages	Discharge P (psia)
1	16.7	8	2216
2	67.0	6	2216
3	300.1	4	2216
4	600.2	4	2216

Ninety seven (97)% mechanical efficiency was assumed in all simulations. The compressor quotes included an undisclosed mechanical efficiency. Covered impellers were assumed for stages less than 400 mm in diameter. An intercooler temperature was given in the compressor quotes and was used in the simulations; however, the intercooler temperature for the last stage or two was not provided. In the simulations for the first two compressors, no intercoolers were used before the last stage. In the simulations for the third compressor, no intercooler was used before the last two stages. In the fourth case, no intercooler was included before the last three stages. The overall efficiency was calculated using a stage power weighted average. Table 38 shows the results of the simulations compared to the compressor quotes.

Table 4: Comparison of Simulations to Compressor Quotes

	Power % Err (%)	Discharge P % Err (%)	Discharge T Diff (°F)	Efficiency Diff (pp)
1a	5.39	-0.89	9.4	0.88
1b	5.88	0.00	10.2	0.68
2a	5.81	6.74	12.4	-0.33
2b	3.08	0.00	-6.8	-0.12
3a	-0.09	-0.21	10.6	0.78
3b	-1.79	0.00	-3.12	0.95
4a	0.75	9.12	11.82	0.46
4c	-6.11	0.00	1.85	0.83

From Table 38 it appears that the simulation provides reasonable results for the integral gear case. All results are within 10% of the compressor quotes.

7.2 Results for Typical Feed

Two types of compressors, integral gear and inline, were compared for a typical CO_2 stream from a solid sorbent capture process at a 650 MW coal-fired power plant. The compressors were assumed to have a combined mechanical/driver efficiency of 97%. Covered impellers were used for stages with diameters less than 400 mm, otherwise open impellers were used. The comparison includes a TEG drying system that reduces the water content of the CO_2 to 150 ppm on a mole basis. All intercoolers were assumed to cool to 104°F with a pressure drop of 1.45 psi. The drying system was assumed to have a pressure drop of 5 psi.

Table 39 shows the inlet and outlet conditions of the compressors. The CO_2 stream represents half of the total flow from the capture process.

Table 5: Solid Sorbent Capture, CO_2 Stream Conditions

	Inlet	Outlet
Flow Rate (lbmol/hr)	12,530	11,780
Temperature (F)	104	104
Pressure (psia)	14.68	2216
Mole Fraction CO_2	0.94000	0.99985
Mole Fraction Water	0.06000	0.00015

Table 40 provides a summary of the simulation results for each type of compressor. Although the compressor designs are not optimized, there should be a reasonable comparison.

Table 6: Compressor Comparison Summary

	Integral Gear	Inline
Total Power (kW)	24,972	29,717
Average Polytropic Efficiency (%)	84.7	84.0
Total Cooling (kW)	44,897	48,708.2
Dryer Reboiler Duty (kW reboiler at 250°F)	786	1,341
Recoverable Heat (kW above 250°F)	902	23,547.4
CO_2 Recycle (%)	2.25	3.0

The following two sections provide more detailed information for the two compressors.

Integral Gear

Table 41 summarizes the results of each stage in the integral gear compressor simulation. This simulation is saved as "CompIG.acmf," which can be accessed for detailed results.

Table 7: Integral Gear Compressor Stage Summary

Stage	η_p (%)	Power (kW)	T_s (F)	T_d (F)	P_s (psia)	P_d (psia)
Compress 1	85.7	4,984.1	104.0	239.8	14.7	35.7
Cool 1	--	--	239.8	104.0	35.7	34.3
Compress 2	82.7	4,736.2	104.0	240.2	34.3	80.0
Cool 2	--	--	240.2	104.0	80.0	78.5
Compress 3	85.7	3,739.7	104.0	215.9	78.5	162.4
Cool 3	--	--	215.9	104.0	162.4	160.9
Compress 4	84.1	3,344.9	104.0	208.3	160.9	312.2
Cool 4	--	--	208.3	104.0	312.2	310.8
Compress 5	85.8	2,510.1	104.0	188.7	310.8	536.0
Cool 5	--	--	188.7	104.0	536.0	534.6
Compress 6	84.3	2,162.9	104.0	184.7	534.6	888.3
Cool 6	--	--	184.7	104.0	888.3	886.8
Dry	--	--	104.0	104.0	886.8	881.8
Compress 7	85.8	1,678.3	104.0	186.0	881.8	1,429.6
Compress 8	84.1	1,815.3	189.0	259.7	1,429.6	2,217.5
Cool 8	--	--	259.7	104.0	2,217.5	2,216.0

Inline

Table 42 summarizes the results of each stage in the inline compressor simulation. This simulation is saved as "CompInline.acmf," which can be accessed for detailed results.

Table 8: Inline Compressor Stage Summary

Stage	η_p (%)	Power (kW)	T_s (°F)	T_d (°F)	P_s (psia)	P_d (psia)
Compress 1	85.9	4,273.5	104.0	222.2	14.7	31.6
Compress 2	84.3	4,462.5	222.2	338.8	31.6	61.3
Compress 3	80.7	4,586.6	338.8	453.6	61.3	107.8
Cool 1	--	--	453.6	104.0	107.8	106.3
Compress 4	85.7	2,774.0	104.0	189.3	106.3	185.3
Compress 5	85.5	2,890.6	189.3	274.8	185.3	307.9
Compress 6	83.4	2,953.5	274.8	359.5	307.9	484.2
Compress 7	80.8	3,010.3	359.5	443.2	484.2	725.3
Cool 2	--	--	443.2	104.0	725.3	723.8
Dry	--	--	104.0	104.0	723.8	718.8
Compress 8	85.7	1,545.5	119.0	186.0	718.8	1,081.6
Compress 9	85.8	1,596.6	186.0	251.3	1,081.6	1,578.4
Compress 10	84.8	1,624.4	251.3	312.9	1,578.4	2,217.5
Cool 3	--	--	312.9	104.0	2,217.5	2,216.0

8.0 DYNAMIC SIMULATIONS

The integral gear compressor offers high efficiencies and relatively low power requirements for CO_2 compression systems in comparison to the inline compressors. Therefore, integral gear compressors have been considered while developing dynamic models for the off-design conditions. The integral gear design consists of pairs of stages arranged around a central gear. Both stages in a pair operate at the same speed but can have different diameters. Since the rotation speed changes after every other stage, stages can operate near their optimum efficiency. The arrangement of an integral gear compressor also allows intercooling after every stage, which significantly reduces the power requirement. At high pressure, intercooling is reduced or not used at all to avoid liquefaction of CO_2. Due to the intercooling, temperatures do not generally get high enough to recover compression heat for use in other parts of the process. The high pressure discharge stream from the compressor is cooled in a water cooler and then sent to a flash drum to separate water from the gas stream. The Aspen Plus blocks of heater and flash drum are imported into the ACM for this purpose. For each compressor stage, a recycle valve has been modeled. A portion of the vapor stream coming from the flash vessel is used as the recycle stream to the compressor inlet. During the normal operating conditions, these valves remain closed. It is assumed that the flow rate of the recycled CO_2 stream to the compressor inlet is regulated by throttle valves. Equation 14 is used to model these valves (Turton, et al., 2012).

$$Q = C_v f(x) \sqrt{\frac{\Delta P}{\rho}} \tag{14}$$

In the above equation, Q represents the volumetric flow rate, C_v represents the valve coefficient, $f(x)$ is the inherent flow characteristic of the valve, ΔP is the pressure drop across the valve, and ρ is the density of the flowing stream. Valve coefficients are calculated assuming 50% opening and 15 psi pressure drop at the surge condition. In real life systems, quite often a quick acting valve is used when the compressor is at close proximity to the surge limit line, while an equal percentage valve is used when the compressor operates above the surge control line. It can be noted that $f(x) = \sqrt{x}$ for a quick opening valve and $f(x) = D^{x-1}$ for an equal percentage valve, where D is a design parameter. The TEG drying system was modeled to remove the water further. The absorber and regenerator consist of packed columns.

8.1 Performance Curves

The performance curves received from a commercial vendor as per specifications have been used. The extracted data from the performance curves have been converted into dimensionless exit flow coefficient (Ψ_3) and non-dimensional impeller isentropic head coefficient (Ψ_s) so the performance curves can be applied to wide variations in Ma number and inlet operating conditions (Lüdtke, 2004). The CO_2 compression system model is updated to evaluate the same dimensionless numbers.

The experimental performance curves contained the data of suction flow rate and discharge pressure. For the first stage, the performance curves have been provided with inlet guide vanes (IGV) for regulating the load. For all the other stages, the curves are without IGV.

The dimensionless exit flow coefficient is calculated using the suction flow rate (V_s) (Equations 15–17)

$$\varphi_3 = \frac{\dot{V}_3}{\pi d_2 b_2 u_2} \tag{15}$$

where, $\dot{V}_3$ = Static volumetric flow rate at impeller exit (m^3/s)

d_2 = Impeller diameter (m)

b_2 = Impeller exit width (m)

u_2 = Impeller tip speed (m/s)

$\dot{V}_3$ can be calculated based on suction flow rate

$$\dot{V}_3 = \dot{V}_s \frac{z_d T_d P_s}{P_d z_s T_s} \tag{16}$$

where, $\dot{V}_s$ = Static volumetric flow rate at the suction (m3/s)

z_s, z_d = Compressibility factor at suction and discharge respectively (dimensionless)

P_s, P_d = Pressure at suction and discharge respectively (bar)

T_s, T_d = Temperature at suction and discharge respectively (K)

$$T_d = T_s \left(\frac{P_d}{P_s}\right)^{\frac{k-1}{k\eta}} \tag{17}$$

where, k = Isentropic volume exponent (dimensionless)

η = Polytropic impeller efficiency (dimensionless)

The dimensionless isentropic head coefficient is calculated using the pressure ratio (Lüdtke) (Equations 18–19)

$$\varphi_s = \frac{2y_s}{u_2^2} \tag{18}$$

where, y_s = Isentropic head = $z_s R T_s \frac{k}{k-1}\left(\left(\frac{P_d}{P_s}\right)^{\frac{k-1}{k}} - 1\right)$ (19)

The impeller diameter and tip speed are calculated by using the code developed previously. The dimensionless performance curves are shown below. Figure 76 represents the performance curves of Stage 1 for different IGV openings. The legends in the figure represent the angle of the vanes. The X-axis

represents the dimensionless inlet flow coefficient and the Y-axis represents the dimensionless isentropic head coefficient. For all the performance curves, correlations have been developed between φ_3 and φ_s using the curve fitting tool box in MATLAB® (Equation 20). The form of the correlation developed is

$$\varphi_s = A\varphi_3^2 + B\varphi_3 + C \tag{20}$$

where, A, B, and C are the estimated fitting parameters. The model results match well with the experimental values. The estimated parameters for all the angles are shown in Table 43.

Table 9: Estimated Parameters for Stage 1

Angle	A	B	C	R^2
-15	-40.73	8.019	0.8982	0.9986
0	-38.87	7.161	0.9519	0.999
15	-37	6.175	1.015	0.9989
30	-36.43	5.384	1.063	0.9983
40	-36.65	4.703	1.113	0.9985
50	-40.02	4.479	1.132	0.9984
60	-68.55	9.451	0.8549	0.9999
70	-127.6	18.04	0.4634	0.9996
75	-191.1	26.35	0.1425	0.9996

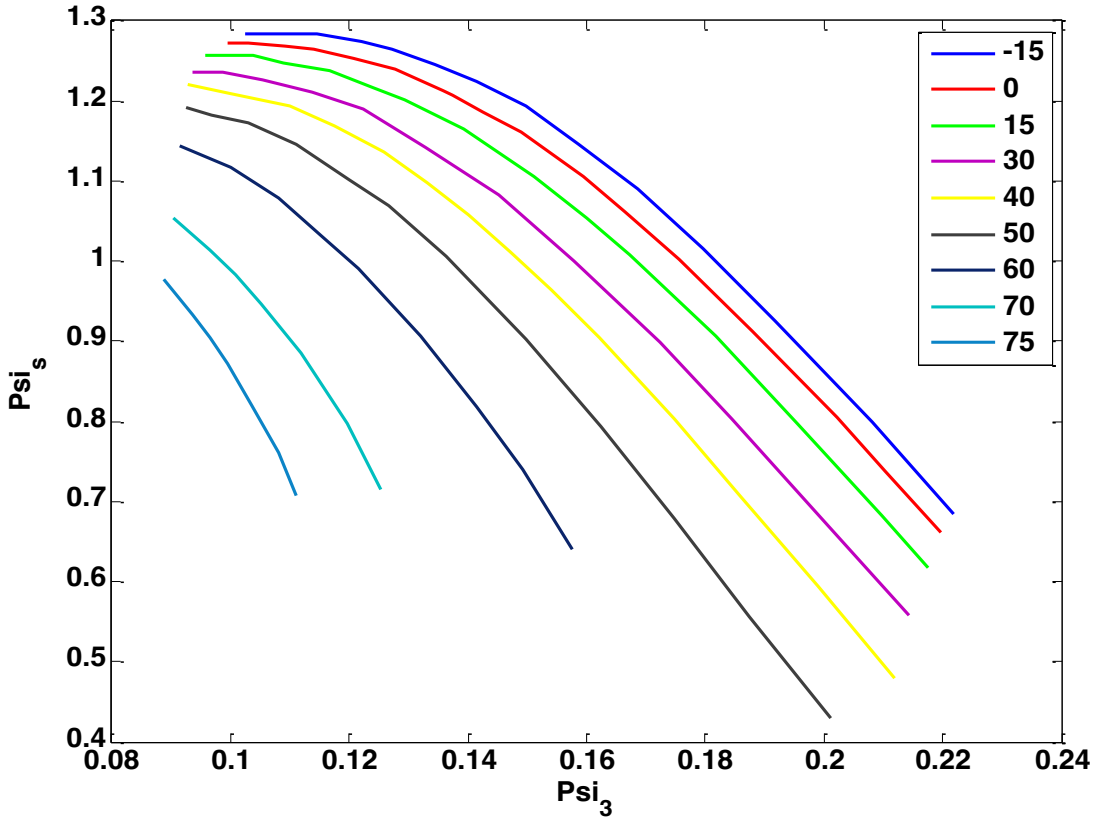

Figure 8: Dimensionless performance curves for Stage 1.

The load can be controlled by manipulating the angle of IGV in the first stage. For this purpose, correlations have been developed between angle and A, B, and C (Equation 21). The proposed correlations are of the form

$$y = ae^{bx} + ce^{dx} \tag{21}$$

where, y = A/B/C and x = angle and a, b, c, and d are the estimated parameters. The estimated parameters for the above correlation are shown in Table 44.

Table 10: Estimated Parameters for Correlation 21

y	a	b	c	d
A	-38.46	-0.005098	-0.1043	0.09821
B	6.863	-0.01329	0.02018	0.09443
C	-0.00891	0.06757	0.9661	0.006228

A similar estimation technique is followed for other stages. The regressed parameters corresponding to Equation 20 are shown in Table 45.

Table 11: Estimated Parameters for Stages 3, 5, and 7

Stage	A	B	C	R^2
3	-33.47	6.619	0.9557	0.9994
5	-28.5	6.457	0.9217	0.9996
7	-16.04	4.986	0.6715	0.9998

8.2 Surge Line

Surge condition is one of the undesirable operating conditions of the compressor. The flow would be reversed under surge conditions. Due to fluctuations in pressure and flow, the compressor operation becomes unstable. Hence, for smooth operation, the suction flow rate should be away from the surge limit line. In general, the minimum suction flow rate is about 10% away from the surge line. This line on the performance curve is called the surge control line. If the operating suction flow crosses this point, it indicates that the system is approaching the surge point. Under these conditions, the recycle valves will be opened to recycle some of the flow to the suction so the system moves away from the surge. To detect the surge approach conditions of a compressor, a robust algorithm is needed so the control system takes the action quickly (Equation 22). The condition for the system surge is

$$\frac{\partial}{\partial \dot{V}}\left({}^{P_d}/_{P_s}\right) = 0 \tag{22}$$

For a more generalized form, the above equation is represented in the dimensionless parameters (Equation 23). The surge point in terms of the dimensionless parameters is

$$\frac{\partial \varphi_s}{\partial \varphi_3} = 0 \tag{23}$$

As the first stage of the compressor is with IGVs, surge conditions vary depending on the IGV angle. These points can be represented on a straight line (Equation 24). The equation of the surge line for the first stage is

$$\varphi_s = 3.684281\varphi_3 + 0.9051 \tag{24}$$

For all the other stages, the surge condition is just a point. PID controllers with gain scheduling have been designed for surge control. For these controllers, controlled variable is proximity to surge, and the manipulated variable is the recycle valve opening (Equation 25). The proximity to surge (PS) is defined as:

$$PS = \frac{\varphi_3^{op} - \varphi_3^*}{\varphi_3^*} \tag{25}$$

where, φ_3^* = Dimensionless inlet flow coefficient at surge point

φ_3^{op} = Dimensionless inlet flow coefficient at the current operating point

The gain-scheduling controller was developed using an adaptive λ-tracker control law (Ilchman, 1993, and Ilchman and Ryan, 1994). This law drives the output to zero with a prescribed tolerance level. This tolerance is introduced together with a dead zone since no action is needed, as *PS(t)* moves beyond the surge control line. First the following function is defined (Equation 26):

$$\sigma_\lambda(\xi) = \begin{cases} 0 & if\ 0 \le \xi \le \lambda \\ \xi - \lambda & if\ \xi > \lambda \end{cases} \tag{26}$$

Then the following adaptive control law is applied (Equation 27):

$$\begin{aligned} u(t) &= k(t)y(t) + u_0 \\ k(t) &= \alpha\sigma_\lambda\left(|y(y)|\right) \\ k(0) &= k_0 \end{aligned} \tag{27}$$

Here *k(t)* is the adaptive gain and α represents the adaptation speed.

ACM Dynamic Simulation

1. For running the dynamic models ACM Version 14 is required for compatibility with the properties model (i.e., the properties definition file teg4dyn.appdf is version dependent even though the ACM model is agnostic to the specific version of ACM.
2. Open the folder named “CO2_COMPRESSION_SYSTEM/Dynamic.”
3. Load “CompIG.acmf.”
4. The first time the model is loaded in a machine, it does not know the path to the properties file. A message displays that reads: “Unable to load file. Do you want to edit properties?” Click “Yes.” This opens a window with a number of options for the properties file. Click “Use Properties Definition File” under “Use Aspen Property System” option. At the next dialog, browse to the folder “CO2_COMPRESSION_SYSTEM/Dynamic/,” select the file named “teg4dyn,” click “Open,” and then click “OK.” This opens the “Physical Properties Configuration” window. The properties status shown at the bottom of this window should be green. Click “OK.” Now the ACM model should load.
5. When the file is loaded, it will issue the following warning in the message window: “159: Upper as IntegerParameter; Warning at position 7…….” This warning can be disregarded as “Upper” has not been used as a variable inside any model, but simply a Global variable that simply appears in the AllGlobals table.
6. Load snapshot “Initial.”
7. Run → “Dynamic.”
8. A warning is issued in the message window: “Warning: Eq_2092_Blocks(“Stripper”).BackFlow.F is near singular, ……” This warning is generated from the Stripper block, which is an Aspen native RadFrac block and by default has these variables for calculating backflow if reverse flow is active. Since reverse flow is not considered in these models, this warning can be safely ignored.
9. Navigate to “Flowsheet” → double-click the plots “Pressure,” “Flow,” “Temperature,” etc.

In the following example, the dynamic model mentioned above is augmented with a script to automatically initiate a ramp change in CO_2 flow rate.

Dynamic Simulation Example: Ramp Change in Inlet Flow Rate

1. For running the dynamic models ACM Version 14 is required for compatibility with the properties model (i.e., the properties definition file teg4dyn.appdf is version dependent even though the ACM model is agnostic to the specific version of ACM.
2. Open "CO2_COMPRESSION_SYSTEM/Dynamic/Example_Flowrate."
3. Load "CompIG.acmf."
4. The first time the model is loaded in a machine, it does not know the path to the properties file. It displays a message that reads: "Unable to load file. Do you want to edit properties?". Click "Yes." This opens a window with a number of options for the properties file. Click "Use Properties Definition File" under "Use Aspen Property System" option. At the next dialog, browse to the folder "CO2_COMPRESSION_SYSTEM/Dynamic/Example_Flowrate," select the file named "teg4dyn," click "Open," and then click "OK." This opens the "Physical Properties Configuration" window. The properties status shown at the bottom of this window should be green. Click "OK." Now the ACM model should load.
5. As before, when the file is loaded, it will issue the following warning in the message window: "159: Upper as IntegerParameter; Warning at position 7……." This warning can be disregarded as "Upper" has not been used as a variable inside any model, but simply a Global variable that simply appears in the AllGlobals table.
6. Load snapshot "Initial."
7. Run → "Dynamic" (Ramp change in flow rate starts at 10 hrs and ends at 13hrs. Simulation stops at 50 hrs.).
8. A warning is issued in the message window: "Warning: Eq_2092_Blocks("Stripper").BackFlow.F is near singular, ……" This warning is generated from the Stripper block, which is an Aspen native RadFrac block and by default has these variables for calculating backflow if reverse flow is active. Since reverse flow is not considered in these models, this warning can be safely ignored.
9. Navigate to "Flowsheet" → double-click the plots "Pressure," "Flow," "Temperature," etc.
10. Observe the following plots in Figures 77–80.

Pressure

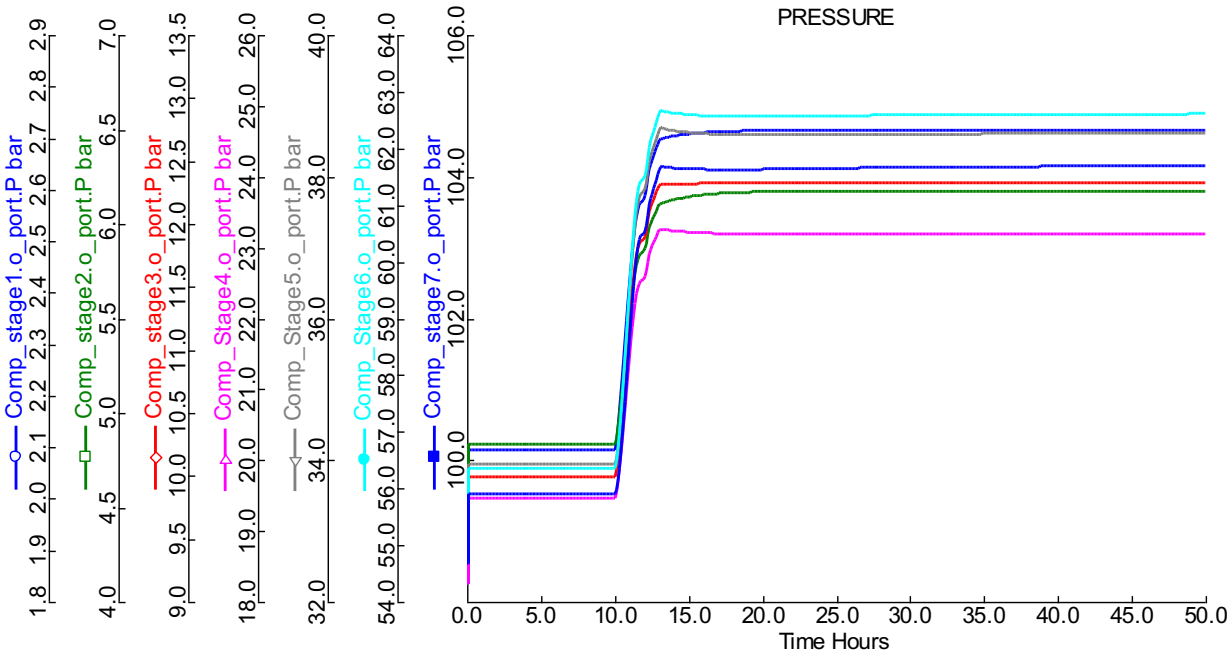

Figure 9: ACM dynamic simulation example: Ramp change in inlet flow rate, pressure plot.

Flow Rate

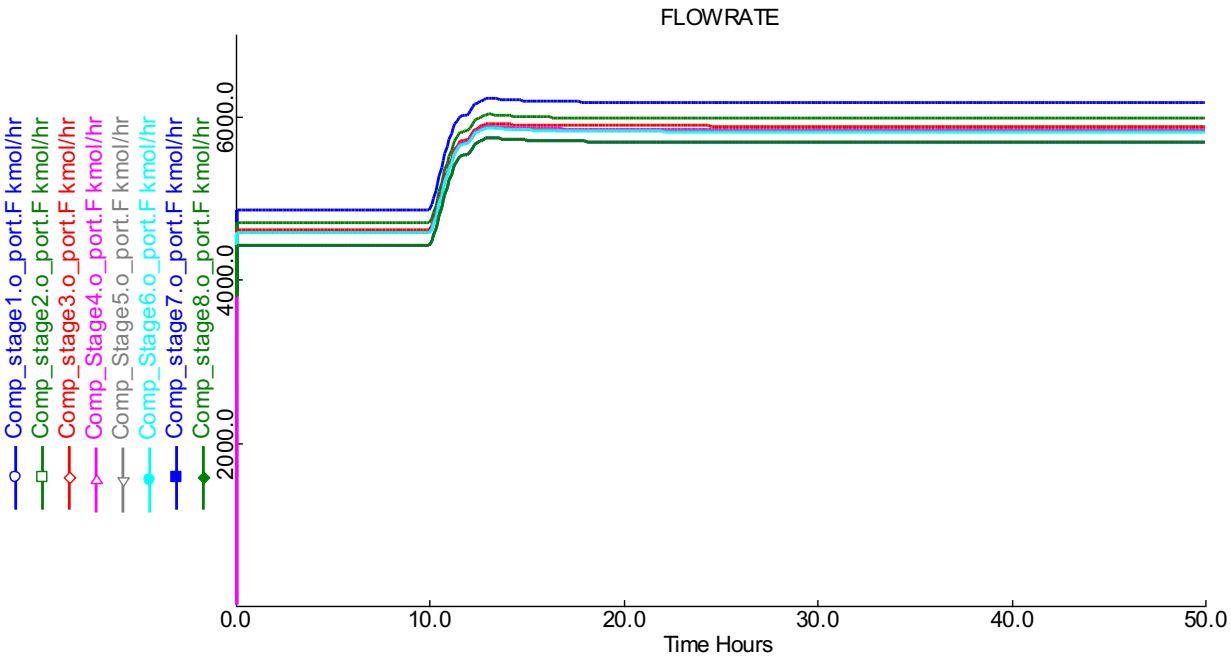

Figure 10: ACM dynamic simulation example: Ramp change in inlet flow rate, flow rate plot.

Temperature

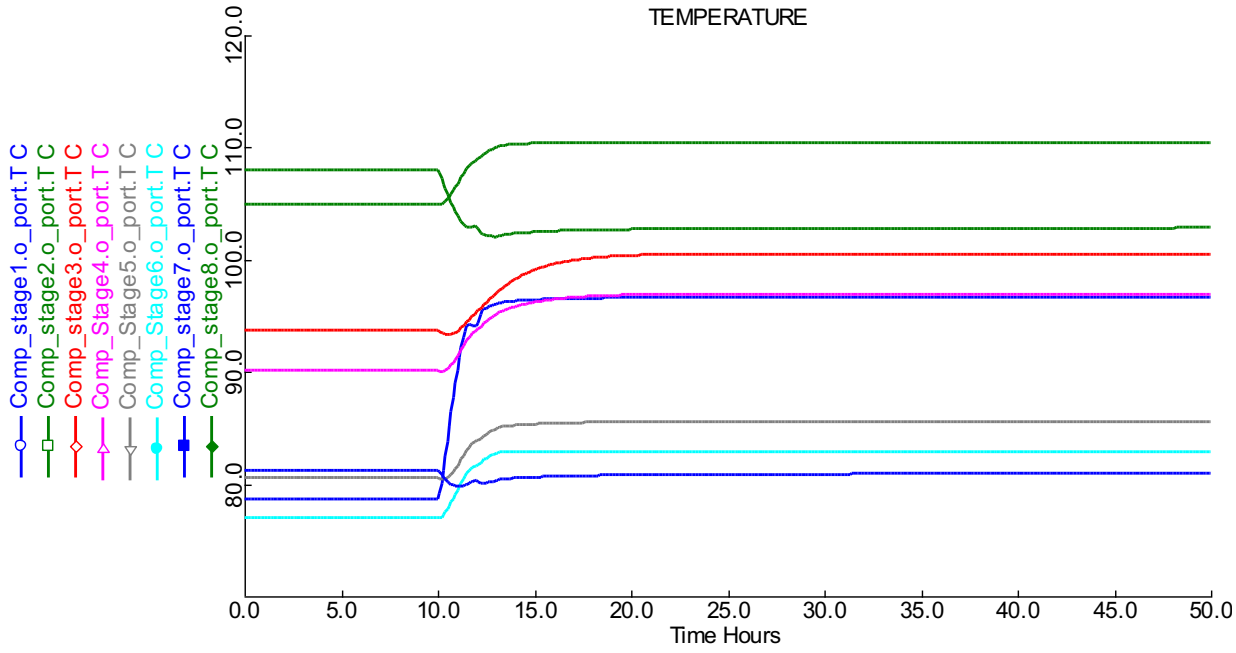

Figure 11: ACM dynamic simulation example: Ramp change in inlet flow rate, temperature plot.

Electric Power

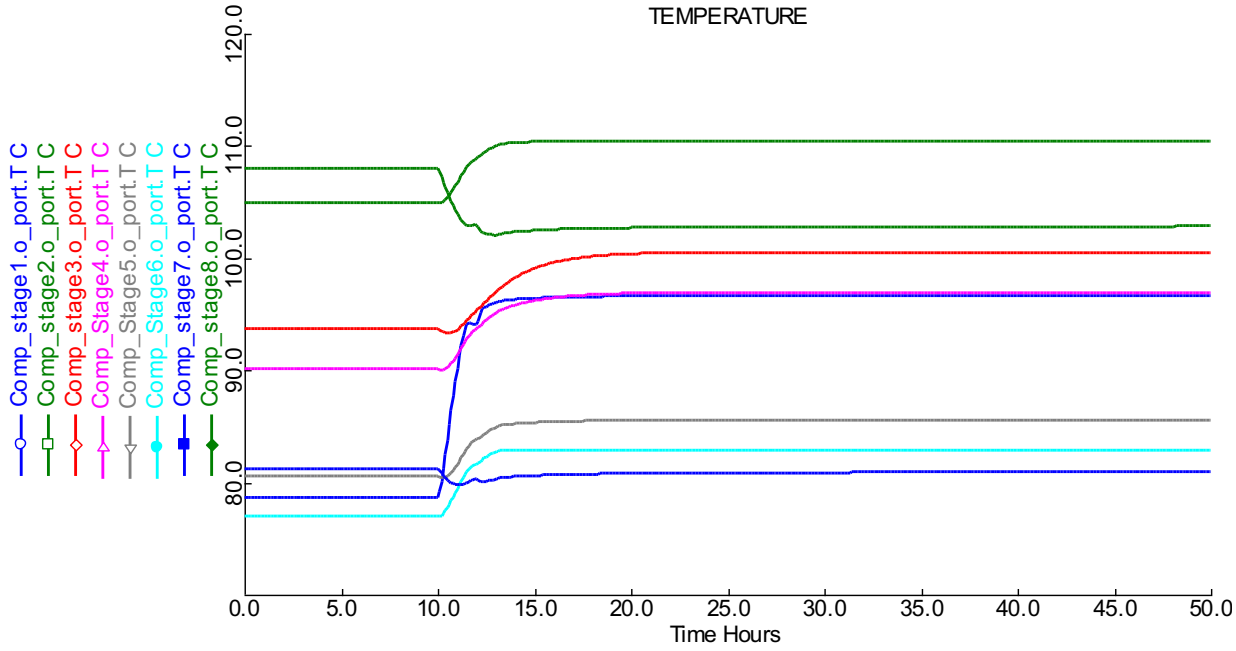

Figure 12: Dynamic simulation example: Ramp change in inlet flow rate, electric power plot.

gPROMS Dynamic Simulation

1. Open the folder named "CO2_COMPRESSION_SYSTEM/DYNAMICS/gPROMS/Flowrate_example."
2. Open "Comp_CO2_ramp.gpj."
3. The compressor model utilizes the built in PML libraries in gPROMS. Navigate to "File" → "Open/Close Libraries." A window opens with a list of available models. Select the "PML libraries" check box and then click "OK."
4. In the "project tree" on the left, navigate to "Comp_CO2_ramp" models and then double-click "CO2_process_flowsheet_full" (see Figure 81).

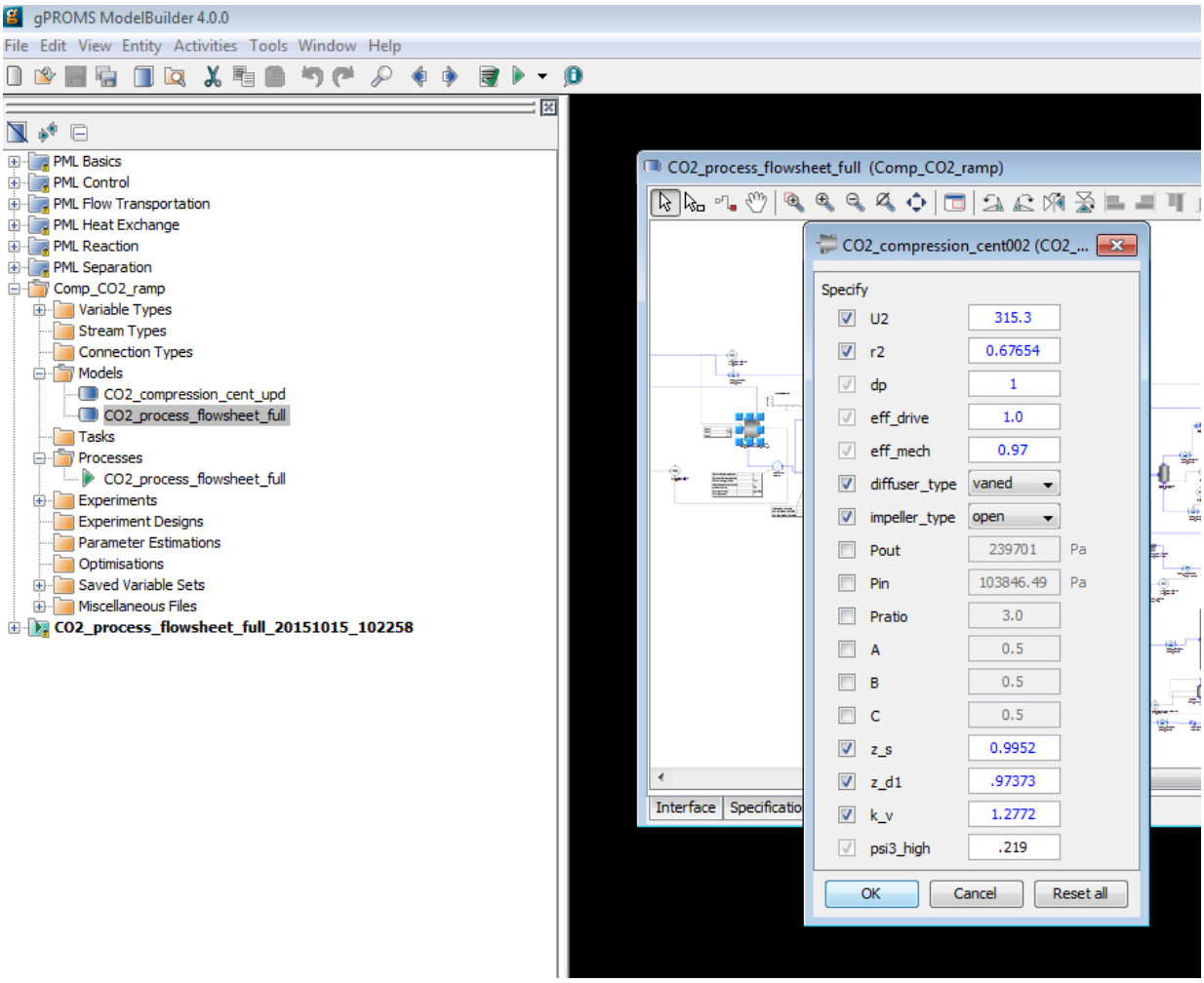

Figure 13: Specification box for compressor model. The process flowsheet model "CO2_process_flowsheet_full" is highlight in the "project tree" menu on the left. Note: Specifying the required variables is done by double-clicking each piece of process equipment under the "Topology" tab of the "CO2_process_flowsheet_full" window. These values are set to default values.

5. Run the model by clicking “Play” (the green button on the top of the toolbar). The “Simulate” option menu displays. Be sure the check box for “Use steady-state initial conditions” is cleared (see Figure 82). The model is setup to automatically select initial conditions. Additionally, be sure to select the “Send results trajectory to gRMS” check box. This sends the results of the simulation to gPROMS data management software, where templates for plotting the results have already been provided. Lastly, ensure that the “Ignore schedule and intrinsic tasks” check box is left cleared. This runs the schedule already set up (it introduces a disturbance) which can be viewed by opening the “CO2_process_flowsheet_full” under the “Processes” folder in the “project tree” and then navigating to the “Schedule” tab. Select the check box to run a steady-state simulation. The disturbance configured is a decrease of inlet flue gas by closing the valve opening.

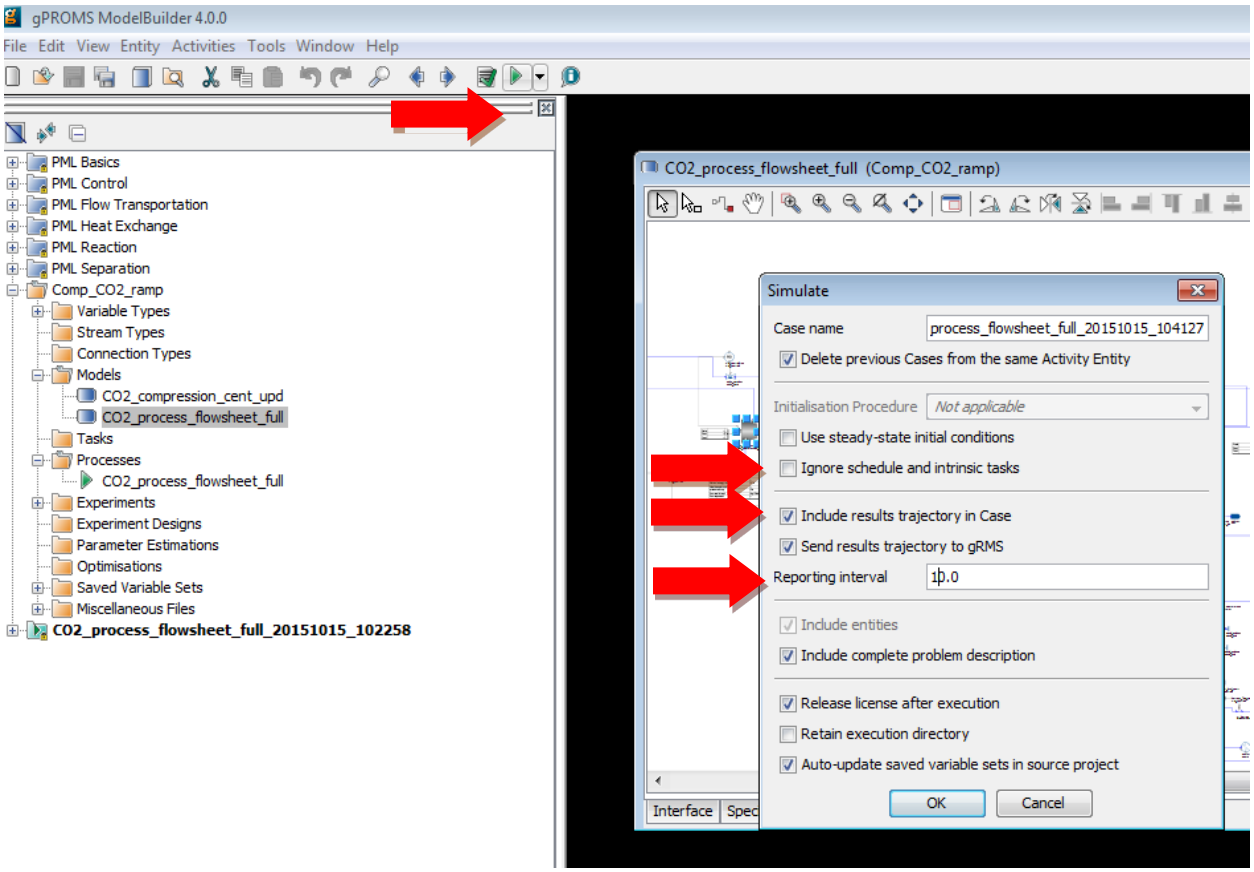

Figure 14: Click “Play” (the green arrow on the top toolbar while the “CO2_process_flowsheet_full Model” window is open). This opens the “Simulate” window. The “Initialisation Procedure” drop-down menu enables the user the option to run the initialization procedure.

6. Click “OK” on the “Simulate” options window to begin the simulation.
7. A new results window displays (listed at the bottom of the “project tree”).
8. A ramp change occurs at 10,000s and the simulation time is 107,200s.
9. To view results, navigate to the “gRMS” window that displayed once the simulation is running. gRMS is a data management program with numerous options and the ability to save a template for the plots, allowing plots to be generated quickly for new simulation results. Four of these templets’ have been provided as “.gpt” files; “elect_power.gpt,” “temperature.gpt,” “pressure.gpt,” and “inlet_gas_flowrate.gpt.” In the “gRMS” window, navigate to “Graph” → “Open Template” and then select the desired template that has been provided. A window displays asking to specify what results the user would like to plot (see Figure 83). Select the “CO2_process_flowsheet_fullxxxxxx_xxxxx” data that is currently being generated. The results will be plotted. Assuming the simulation has not completed running yet, the plots will automatically update as the simulation is solved in gPROMS.

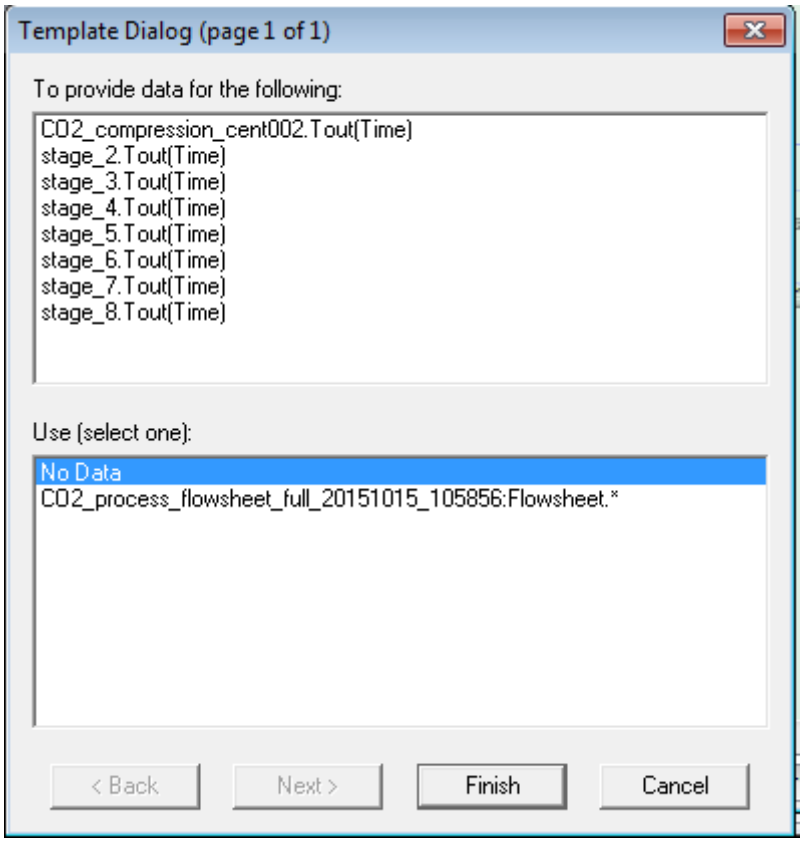

Figure 15: Data selection window for gRMS template.

Note: Results can also be viewed by navigating to the “Trajectories” → “Flowsheet” folder in the results file that is generated at the bottom of the “project tree.” Simply navigate to the desired variable within the flowsheet.

10. When the simulation completes, the results of each template provided are given in Figures 84–87.

Pressure

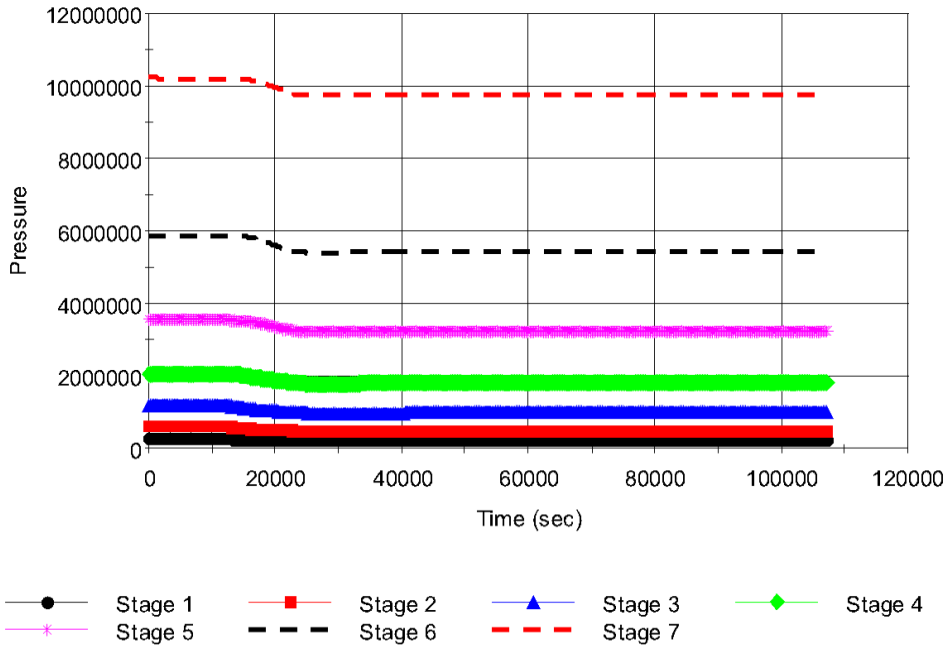

Figure 16: gPROMS dynamic simulation example: Ramp change in inlet flow rate, pressure plot.

Inlet Gas Flowrate

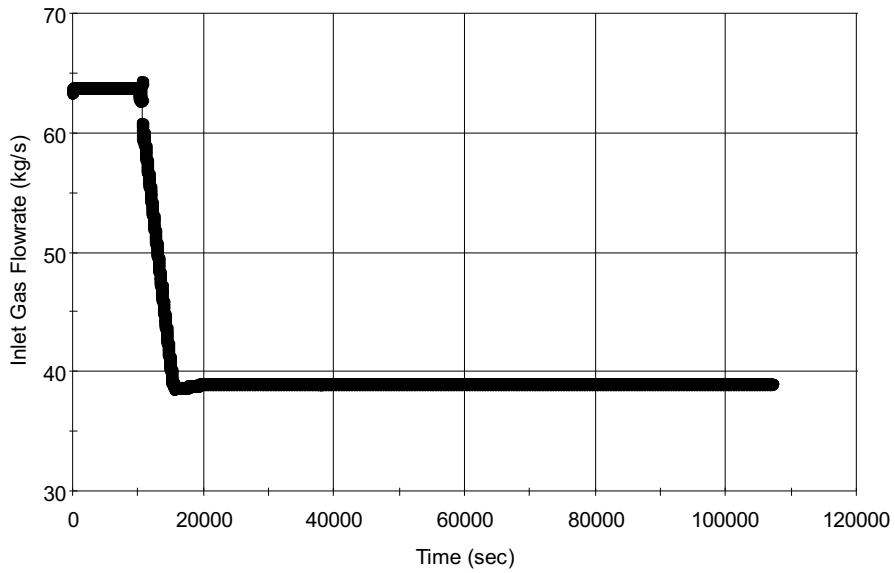

Figure 17: gPROMS dynamic simulation example: Ramp change in inlet flow rate, flow rate plot.

Temperature

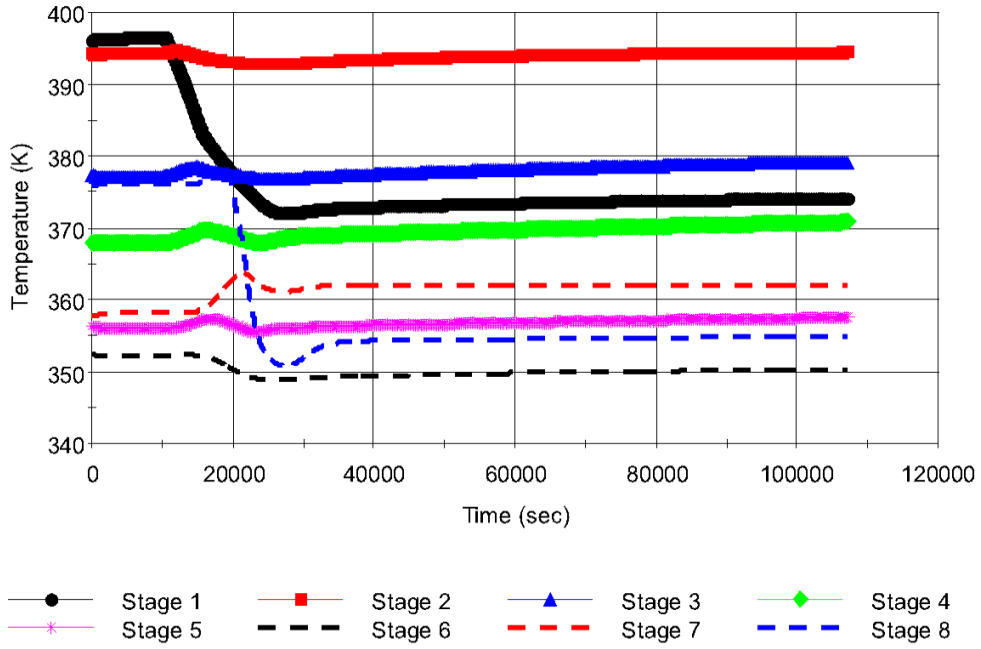

Figure 18: gPROMS dynamic simulation example: Ramp change in inlet flow rate, temperature plot.

Electric Power

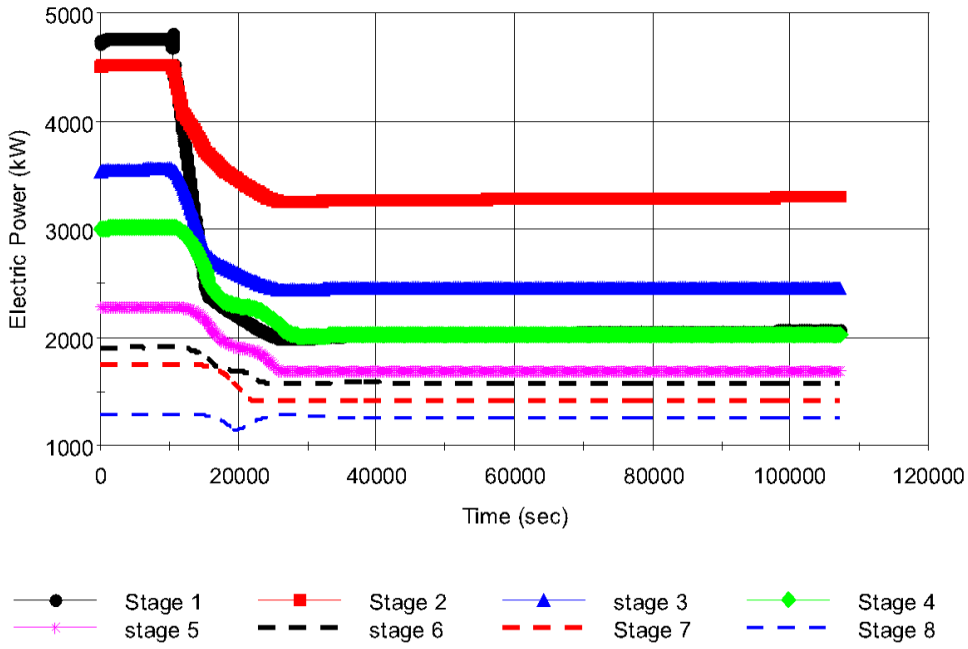

Figure 19: gPROMS dynamic simulation example: Ramp change in inlet flow rate, electric plot.

9.0 REFERENCES

Aungier, R.H. (2000), "Centrifugal Compressors: A Theory for Aerodynamic Design and Analysis," ASME Press, NY.

Ilchman, A. (1993), "Non-Identifier-Based High-Gain Adaptive Control," Springer, NY.

Ilchman, A., and Ryan, E.P. (1994), "Universal λ-Tracking for Nonlinearly Perturbed Systems in the Presence of Noise," Automatica, 30, 337-346.

Kohl, A.L., and Nielson, R. (1997), "Gas Purification," 5th Ed., Gulf Publishing Company, Houston, TX.

Lüdtke, K.H. (2004), "Process Centrifugal Compressors: Basics, Function, Operation, Design, Application," Springer, Berlin.

Lüdtke, K.H., "Twenty Years of Experience with a Modular Design System for Centrifugal Process Compressors," Proceeding of the Twenty-First Turbomachinery Syposium.

Mallen, M., and Saville, G. (1977), "Polytropic Processes in the Performance of Prediction of Centrifugal Compressors," Institute of Mechanical Engineers, Paper No. C183/77.

Span, R., and Wagner, W. (1996), "A New Equation of State for Carbon Dioxide Covering the Fluid Region from the Triple-Point Temperature to 1100 K at Pressures up to 800 MPa," *Journal of Physical Chemistry Reference Data*, v25, 1509-1596.

Turton, R., Bailie, R.C., Whiting, W.B., Shaeiwitz, J.S., Bhattacharyya, D. (2012), "Analysis, Synthesis and Design of Chemical Processes," 4th Edition, Prentice Hall, 2012.

U.S. Department of Energy (2010), "Cost and Performance Baseline for Fossil Energy Plants Volume 1: Bituminous Coal and Natural Gas to Electricity," DOE/NETL-2010/1397.

Weibe, R., and Gaddy, V.L. (1941), "Vapor-Phase Composition of Carbon Dioxide Water Mixtures at Various Temperatures and Pressures to 700 Atmospheres," *Journal of the American Chemical Society*, v63, 475-477.